DNASER I: Layout and Data Analysis

Claudio Nicolini*, Andrea Marco Malvezzi, Alessandra Tomaselli, Davide Sposito, Giuseppe Tropiano, and Enrico Borgogno

***Abstract*—We present the DNA analyzer (DNASER), a novel bioinstrumentation for real-time acquisition and elaboration of images from fluorescent DNA microarrays. A white light beam illuminates the target sample allowing the images grabbing on a high sensibility and wide-band charge-coupled device camera (ORCA II—Hamamatsu). This high-performance device permits to acquire images faster and of higher quality than the traditional systems. The DNA microarrays images are processed to recognize the DNA chip spots, to analyze their superficial distribution on the glass slide and to evaluate their geometric and intensity properties. Differently form conventional techniques, the spots analysis is fully automated and the DNASER does not require any additional information about the DNA microarray geometry.**

The DNASER hardware and software architecture is illustrated. Preliminary results are shown from experiments performed on real DNA samples.

***Index Terms*—DNA microarray, organic matrix.**

I. Introduction

In biomedicine, the *in vivo* and *in vitro* studies of DNA are performed analyzing images from fluorescence microscopy [1]. Nowadays, improvements in fluorescence microscopy (based on sophisticated laser systems), new oligomers deposition methods, and *ad hoc* pattern recognition algorithms allow automatic massive analysis of DNA samples processing images of microarrays of DNA fragments.

Microarrays are matrix-shaped collections of DNA spots deposited on the surface of a glass or nylon slide. Each spot contains many copies of a single DNA sequence such as gene. Generally, DNA spots are left on the slide using a robotic arm as their dimension (less than 200 μm) does not allow a hand-made positioning.

DNA microarrays [13], [14] allow to interrogate expression of hundreds or thousands of genes simultaneously, both in yeast [15] and in human cells [16]. Gene expression data derived from arrays may be used for gene clustering [17], tissue differentiation [18], and other analysis. Then, DNA microarrays provide a medium for matching known and unknown DNA samples based on base-pairing rules and automating the process of identifying the unknowns.

Manuscript received August 21, 2002; revised September 25, 2002. This work was supported by a grant from the Fondazione Elba. *Asterisk indicates corresponding author.*

*C. Nicolini is with the Department of Biophysical MO Sciences and Technologies, University of Genoa, Genoa 16132, Italy. He is also with Polo Nazionale Bioelettronica, Marciana, Italy, and Fondazione Elba, 00134 Rome, Italy (e-mail: cn.roma@tin.it).

A. M. Malvezzi, A. Tomaselli, D. Sposito, G. Tropiano, and E. Borgogno are with the Department of Biophysical MO Sciences and Technologies, University of Genoa, Genoa 16132, Italy. They are also with Polo Nazionale Bioelettronica, Marciana, Italy, and Fondazione Elba, 00134 Rome, Italy.

Digital Object Identifier 10.1109/TNB.2002.806941

In the last years, the design of DNA microarrays analysis devices has driven the development of specific techniques and instrumentation. Complex co-focal microscope [2] (to focus the laser beam on the sample), samples preparation methods [3] (to deposit spots on the slide), multicolor analysis systems [5] (to compare samples with reference data), image processing routines (to extract samples characteristics), statistic analysis routines [4] (to extract the gene characteristic), and data-bases [6] (to store the categories of genic expression).

Recently, charge-coupled device (CCD) camera technology (Vysis [7]) has replaced the co-focal microsopy. These new systems are faster (there is no glass slide scanning), cheaper (CCD camera are cheaper than laser scan systems), and simpler to realize (it is no required laser beam motion control).

In what follows, we present a new system, the DNASER[1] (equipped with the ORCA II Hamamatsu CCD camera), for the analysis of traditional and innovative DNA microarrays [21]. In Section II, the system hardware architecture and the image processing algorithms for the spots analysis are illustrated. In Section III, preliminary results from experiments performed on a real DNA sample are shown. Finally, the conclusions highlight the results.

II. System

A. Hardware

This section describes how the DNASER works and its main hardware components.

The prototype, thanks to the particular optomecanical structure joined to the high-sensitivity CCD camera, generates wide area images in a single shot using samples with very low fluorescence intensity. That is possible because the sample is illuminated with a beam produced by a white light source. The beam, through a specific optical path, is accurately filtered and focused on the sample and then on the CCD camera sensitive area. A Supervisor PC controls DNA microarray images acquisition and elaboration. Fig. 1 shows the main hardware blocks of the bioinstrumentation.

The illumination system, the optical filter system and the motorized holder blocks constitute the optomecanical components. This part is shown in more detail in Fig. 2.

The light source, 3), a 150-W Xenon lamp, generates a collimated beam through an elliptical reflector, 2). Filters, 4) and 5), eliminate IR and UV components. In this way, one avoids excessive heating and ultimately damage, of the sample. Two interchangeable interference filters, 9) and 9′), are placed between two achromatic doublets, 8), so as to work in parallel illumination conditions. Filters 9) and 9′) are different because

[1]Patent pending

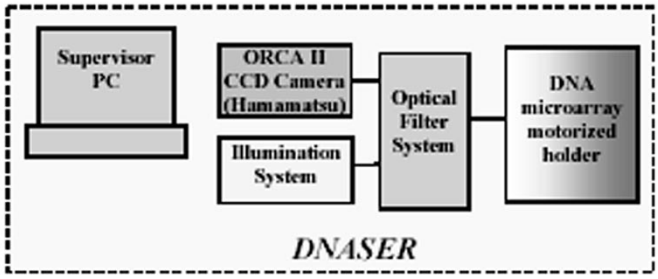

Fig. 1. Block diagram of the DNASER. The illumination system provides a collimated, a wide-band, and a high brilliant white light beam. The optical filter system allows maximizing the information coming out from the sample and strongly reducing noise that does not represent useful information. The DNA microarray motorized holder lets to position the sample on the focal plane of the CCD. The ORCA II CCD camera is able to acquire images fast and of high quality. On the supervisor PC runs the routines devolved to sample fine positioning, image acquiring and spot analysis.

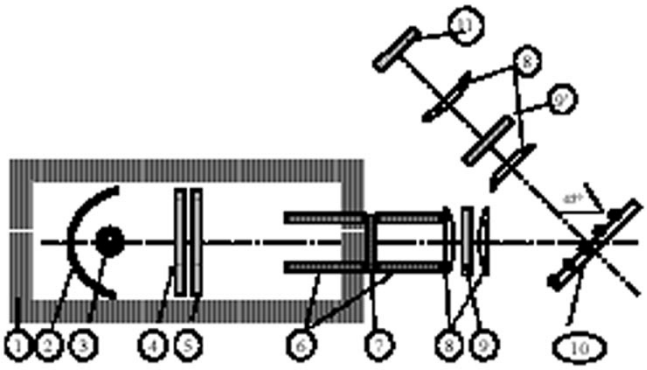

Fig. 2. Optomechanical components of DNASER. 1) Six light shields; 2) elliptical reflector; 3) high-pressure Xe lamp; 4) UV blocking filter; 5) IR blocking filter; 7) iris; 8) achromatic doublets, 9) 9′, interference filters; 10) sample holder on a x-y-z-remotely controlled translation stages, and 11) CCD sensitive area.

are tuned respectively on the excitation and emission frequency of the DNA microarray fluorescent spots. This geometry is used both for illumination of the sample and collection of the fluorescence signal. The spectrally selected light is then focused onto the sample, 10), at 45 degrees of incidence. The illuminated spot dimension is about 1.2×1.2 mm. Three motorized linear translation stages, which are controlled by the computer, are used to fine position the sample on the focal plane (Z axis) of the CCD camera and to select the appropriate portion of area to be imaged (X, Y axis). An *ad hoc* software has been developed in order to position the sample with micrometer precision.

The ORCA II Dual Scan Cooled 12–14 bit B/W CCD Camera combines high-resolution, low noise and high sensitivity, high quantum efficiency, a wide spectral response (300–700 nm) and a high dynamic range (full well capacity of 16.000 electrons and of 40.000 with binning). The camera has two independent clock rates: 1.25 MHz for high-precision imaging, achieving 3–5 electrons read-out noise and 10 MHz for high frame rate imaging. The ORCA II incorporates a CCD with an effective 1280×1024 (1.3 M pixel) pixel array and progressive scan interline design to eliminate the need for a mechanical shutter. The combination of Hamamatu's hermetic vacuum (10-5 torr)

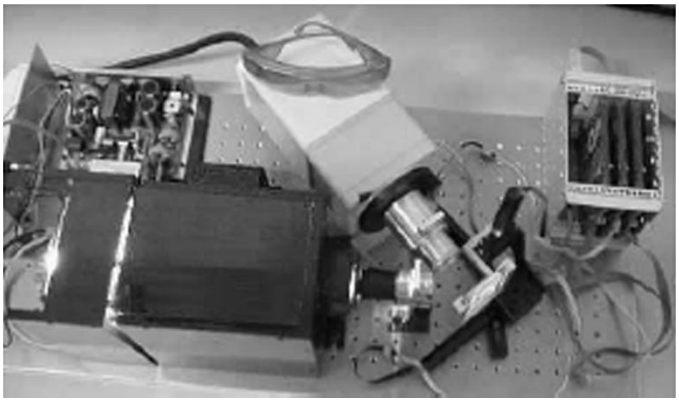

Fig. 3. DNASER prototype.

sealing and Peltier cooling, with air as a heat exchanger, enables the CCD chip to operate at $-50\,^{\circ}$C. This drastically reduces the dark current (0.001 electron/pixel $\times$ s) of the CCD chip. Special analog contrast-enhancement circuits increase versatility for even the most difficult imaging conditions.

The Supervisor PC is Pentium II 233-MHz, 128-MB ram, and 2-GB hard disk.

Fig. 3 shows the actual prototype layout (the PC is not shown).

B. The Software for Spots Analysis

On the supervisor PC runs the software routines (C language) that implement the image processing algorithms for the spot analysis.

Microarrays are built laying spots equidistantly in a grid. While the orientation error of the grid is negligible, its spatial position can significantly vary. Furthermore, depending on the arrayer used, the distance between spots is different. In order to develop a robust system, the image processing algorithm developed to perform the spot analysis estimates these data instead of supposing them given.

The input data to the spot analysis are the raw DNA microarray images. The output data of this processing are all the spot features.

- Brightness features (spot foreground and background intensity).
- Geometric features (spot foreground and background area, circularity).

The microarray geometry suggests to organize the output data using three-dimensional matrices (Fig. 4). The width and height of the matrix are given, respectively, by the number of columns and rows of the spots in the microarray. While, the depth is given by the number of features associated to each spot.

These data structures permit to store the spot features according to the relative positions that they have in the original image. This property allows to perform further microarrays data processing directly using the associated matrices, reducing the computational burden. Also, this data representation is appealing to build an efficient data-base of microarrays features as it permits an intuitive and fast comparison of properties among correspondent spots.

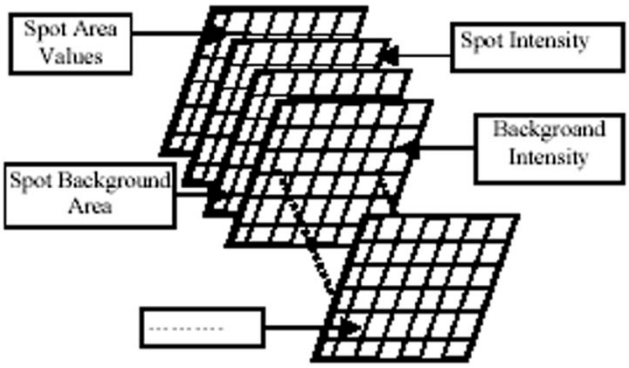

Fig. 4. Spot features organization on 3-D matrix.

Fig. 5. DNA microarray image acquired with the DNASER instrumentation. The image is been equalized to emphasize the noisy.

The spot analysis can be logically divided in the following three main sequential steps:

- image segmentation;
- spot recognition;
- spot features extraction.

In the rest of this section, these algorithms will be illustrated separately.

1) Image Segmentation: The image segmentation processing is aimed to partition the pixels of the microarrays images in two classes: foreground pixels, that are the pixels belonging the microarray spots and background pixels, that are the pixels out of the microarray spots.

The microarrays images are typically very noisy (Fig. 5, Section III). The not-homogenous scene illumination, the light-scattering, and not perfectly cleaned glass slides generate unpredictable variations in the image background intensity and also introduce in the image false foreground entities.

The simplest solution to realize the image segmentation is the definition of a single intensity threshold and the partition of the image in background and foreground pixels according to its value. Indeed, due to the problems mentioned above, to use this approach is required a preelaboration to smooth the intensity variations in the image (rolling-ball algorithm [8]). Alternatively, this preelaboration can be avoided considering more thresholds values evaluated, time from time , according the local intensity distribution in the image.

Microarrays images are typically characterized by intensity distribution that result in unimodal histograms. This property complicates the threshold estimation problem, involving the use of sophisticated techniques. We considered two algorithms to estimate the background/foreground threshold for images (or subimages), both based on the image histogram analysis:

- isodata algorithm [9];
- triangle algorithm [10].

The isodata algorithm addresses the search of the best threshold performing an iterative process on the intensity histogram of the image. In particular, it works considering two main steps.

— At start, the image histogram is divided in two regions (foreground and background) using the initial threshold value θ evaluated as the mean of the whole histogram.

— At each iteration, for both the background and foreground regions defined as in the previous step, are evaluated the mean intensity values, respectively, m_b, m_f. The mean of m_b and m_f is assumed as the new threshold θ and according this value the background and foreground regions are redefined. If the threshold value evaluate in this step is the same, then the one from the previous step the process stops. Otherwise, this step is iterated.

The final value of θ is then assumed as the best threshold value for the considered image.

The Triangle algorithm works directly estimating the threshold value, without generating any iteration. Given the histogram function of the image $h(b)$ ($h(b)$ is the number of pixels characterized by brightness b), a segment is constructed between the maximum of $h(b)$ (at $b = b_1$) and the highest value of b in the image ($b = b_2$). The distance d between the segment and the histogram $h(b)$ is evaluated for all values $b \in [b_1, b_2]$. The value of b where the distance d is maximal is taken as threshold value.

It is of worth to note that, while the Isodata algorithm is a general approach to the threshold estimation problem, the Triangle algorithm has been developed particularly to deal with unimodal histograms.

2) Spots Recognition: The spot recognition algorithm, working on the segmented image, identifies the spots present in the microarray image. In particular, this process can be divided in two main steps.

- Spots preliminary identification: the pixels in the foreground set are partitioned, including in the same subset all the pixels that belong to the same spot. This phase builds the candidate spot set.
- Spots identification refining: the features and position of the spots are used to check their consistency. Also, if this is the case, lost spots are recovered from the background set.

The spots' preliminary identification is performed using a blob analysis technique [11]. This algorithm using neighborhood connectivity rules extracts image blobs (spots), that are isolated groups of pixels in the image. Two main pixels properties drive this processing.

- Neighboring pixels: two pixels such that their Euclidean distance in the image is less than two pixels.
- Boundary pixel: a foreground pixel that has at least one background pixel as neighbor.

If and S_b are, respectively, the foreground and background sets and S_{bl} is the generic blob pixel set, the algorithm works iterating the following steps until S_f is empty.

- Take a boundary pixel p_0 from S_f, add it to S_{bl} and fix a versus v along that boundary.
- Starting with $k = 1$, extract and add to S_{bl} all the pixels p_k evaluate ricorsively as the neighbor boundary pixel of p_{k-1} in the direction v until $p_k \neq p_0$.
- Take all the pixels in S_f that lay inside the contour drawn by S_{bl} and add them to S_{bl}.
- Update S_f erasing all the pixels in S_{bf}.

At each iteration the algorithm extracts one blob, which pixels are stored in the correspondent S_{bl} set. When S_f is empty the collection of blob sets extracted S^1_{bf}, S^2_{bf}, …, S^n_{bf} gives the set of the candidate spots. Blobs made of too little number of pixels are not considered.

The spot identification refining algorithm works on the set of candidate spots performing two sequential elaborations. First, the position of the candidate spots (center of mass of the relative blobs) are evaluated and used to reconstruct the microarray grid, that is, it is evaluated the best set of vertical and horizontal lines, equidistant from the spots and such that just one blob is inside one square (box) of the chess box [Fig. 8(a), Section III]. This grid allows one to check the consistency of the candidate spots: if they are correctly positioned, they are real spots; otherwise, they are noise. Furthermore, if there are no candidate spots in a chess box it means that or the spot is occluded in the image or the pixels of this spot have been classified as background. In the last case, a new segmentation and blob analysis process can be performed, locally, on the image pixels that lay in chess box to try to recover the lost spot.

It is worthwhile to deepen the grid-building task. From our hypothesis, we know that the spots in the microarray image are positioned along horizontal lines and are, to each other, equidistant both horizontally and vertically. The absolute position of the grid is unknown, as is the spot distance, furthermore some spots can miss and others can be due to noise. We approached the problem of clustering the spots (in the candidate set) that are supposed to belong to the same microarray row (a vertical positioning error less than the medium radius of the estimated spots is tolerated). For each row set, the medium and the variance of the elements distances are evaluated and, among the sets with higher cardinality, the grid distance is taken as the medium distance of the set with the smallest variance.

The second step of the identification spot refining algorithm concerns the compatibility of each estimated spot features with both, the expected spot properties and the medium characteristics of the estimated spots. The medium value of the spot surface, spot circularity and positioning error in the grid are evaluated over the set of the estimated spot. These criterion are used to perform a quality check on the estimated spots and, if it is the case, to eliminate not reliable estimation.

3) Spot Features Extraction: Identified all the spots in the microarray images, this processing step is aimed to extract for each spot a set of features. Such analysis allows one to describe the main characteristics of each spot by means of a reduced set of parameters, simplifying the problems of characterizing, storing, and classifying data from microarray images.

If the significant features to extract from spots are strictly dependent on the kind of analysis that is going to be performed, then it is not possible to define a general set of features. For this reason, we have investigated for the features that are considered for almost all the researches. In particular, we considered the following spot features.

- Spot (foreground) area: The number of pixels belonging the correspondent blob of the image.
- Spot background area: The number of background pixels laying in the spot chess box.
- Spot intensity: The average intensity of the correspondent blob.
- Spot background intensity: The average intensity of the background pixels in the spot chess box. Indeed, to reduce noise, only a proper subset of these pixels is considered [12].
- Spot circularity: A measure of the circularity of the correspondent blob in the image.
- Spot position error: The difference between the position of the correspondent blob in the image (its c.o.m.) and the position of the spot chess box center.

All the described features and, if any, other specific once are stored in the 3-D matrix illustrated above.

III. Experiments

In this section, we show the results obtained executing the presented algorithm on a real DNA microarray image acquired with the DNASER instrumentation. Fig. 5 reports the grabbed image.

As mentioned above, the image is very noisy and many spots are barely visible. We execute different segmentation processes on this image to compare their effectiveness. In particular, for both isodata and triangle algorithms, we consider the threshold search on the whole image (I_1), I_1 with rolling-ball preelaboration (RI_1), threshold search considering four subimages (I_4), and I_4 with rolling-ball preelaboration (RI_4).

For both, isodata and triangle methods, cases I_4 and RI_4 performed the best and RI_1 was better then I_1. So the best results, also considering the computational burden, was given by cases I_4. Furthermore, as shown in Fig. 6, isodata I_4 outperformed triangle I_4 and then, in what follow, isodata I_4 is the segmentation algorithm used.

Fig. 7 reports the blobs extracted using the presented blob analysis algorithm. Considering the real microarray structure, it easy to see that the image is corrupted by false and missing spots. Fig. 8(a) shows the estimated grid lines and the effect of

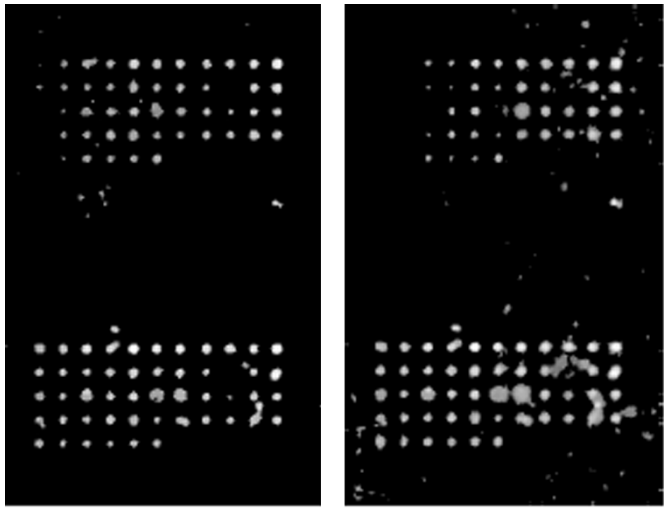

(a) (b)

Fig. 6. (a) Isodata algorithm segmentation; (b) triangle algorithm segmentation.

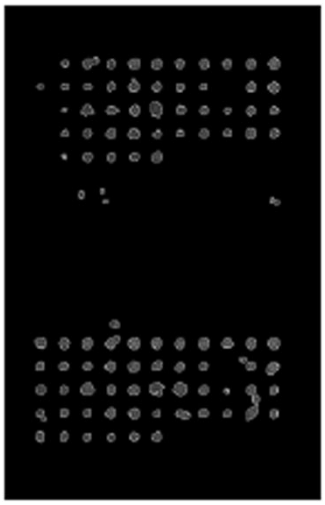

Fig. 7. Blob analysis extraction.

considering the estimated microarray structure to validate the spots consistency. In fact, the false spots in the central part of the image are erased, while the real spots on the first column are recovered. Finally, Fig. 8(b) reports the spots that overcome the criteria of spot quality check.

Blobs in Fig. 8(b) are considered the spots present in the DNA microarray image and for them all the interesting features are extracted and stored in the 3-D matrix.

IV. Conclusion

We presented the DNASER, a new device for the DNA microarrays analysis based on CCD camera technology. The described prototype is a flexible analysis instrument. The special optomecanical instrumentation and the wide-band ORCA II camera allow to acquire DNA microarray images at different frequencies simply changing two different interference filters. The spot analysis algorithm is fully automated and does not require any additional information about the DNA microarray geometry. According to the relative position, the spot features are

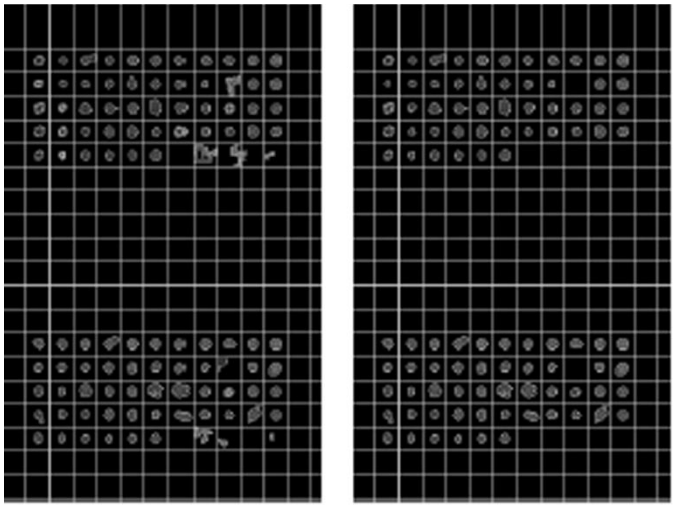

(a) (b)

Fig. 8. (a) Estimate grid lines and spots recovered; (b) spots that overcome the criteria of spot quality check.

stored in a 3-D structure that is appealing to build an efficient database, for classification and further processing purposes.

Preliminary experiments on a real DNA sample showed the different behaviors of the proposed spot analysis techniques and demonstrated the system effectiveness in recognizing and classifying samples.

DNA microarrays analysis devices can be used in the wide range of medical applications that require the DNA study and classification. For example, the DNASER can be used to characterize the cellular differences between different tissue type such us between normal cells and cancer cells at different stages of tumor progression, or between cancers with different responses to treatment, or between control cells and cells treated with a particular drug. To this purpose, our further work is aimed to furnish the system with a database of different microarrays features and to develop, using a neural network, an automatic diagnostic tool for classifying samples on the basis of their gene expression pattern [18], [19].

References

[1] G. Mascetti, L. Vergani, A. Diaspro, S. Carrara, G. Radicchi, and C. Nicolini, "Effect of fixatives on calf thymocyte chromatin: 3D hight resolution fluorescence microscopy," *Cytometry*, vol. 23, no. 2, pp. 110–119, 1996.
[2] O. Hiroshi, U.S. Patent 375 385, Aug. 17, 1999.
[3] D. H. Stewart, J. W. Groelke, H. H. Thorp, and A. E. Eckhardt, U.S. Patent 722 065, Nov. 24, 2000.
[4] J. Ye, C. Yan, V. Di Francesco, and E. M. Beasley, U.S. Patent 800 960, Mar. 8, 2001.
[5] T. D. Harris, R. L. Hansen, W. Karsh, N. A. Nicklaus, and J. K. Trautman, U.S. Patent 724 253, Nov. 28, 2000.
[6] P. F. Davies and D. C. Polacek, U.S. Patent 783 836, Feb. 14, 2001.
[7] D. Che, Patent 049 748, Mar. 27, 1998.
[8] S. Sternberg, "Biomedical image processing," *IEEE Comput. Mag.*, Jan. 1983.
[9] T. W. Ridler and S. Calvard, "Picture thresholding using an iterative selection method," *IEEE Trans. Syst., Man Cybern.*, vol. SMC-8, pp. 630–632, Aug. 1978.
[10] G. W. Zack, W. E. Rogers, and S. A. Latt, "Automatic measurement of sister chromatid exchange frequency," *J. Histochem. Cytochem.*, vol. 25, no. 7, pp. 741–753, 1977.
[11] B. K. P. Horn, *Robot Vision*. Cambridge, MA: MIT Press, 1986, ch. 4.

[12] Y. H. Yang, M. J. Buckley, and T. P. Speed, "Analysis of cDNA microarray images," *Brief Bioinform.*, vol. 2, no. 4, pp. 341–349, Dec. 2001.
[13] M. Schena, D. Shalon, R. W. Davis, and P. O. Brown, "Quantitative monitoring of gene expression patterns with a complementary DNA microarray," *Science*, vol. 270, pp. 467–470, 1995.
[14] C. Nguyen, D. Rocha, S. Granjeaud, M. Baldit, K. Bernard, P. Naquet, and B. R. Jordan, "Differential gene expression in the murine thymus assayed by quantitative hybridization of arrayed cDNA clones," *Genomics*, vol. 29, pp. 207–216, 1995.
[15] S. Chu, J. DeRisi, M. Eisen, J. Mulholland, D. Bottstein, P. O. Brown, and I. Herskowitz, "The transcriptional program of sporulation in budding yeast," *Science*, vol. 282, pp. 699–705, 1998.
[16] C. M. Perou, S. S. Jeffrey, V. van de Rijn, C. A. Rees, M. B. Eisen, D. T. Ross, A. Pergamenschikov, C. F. Williams, S. X. Zhu, J. C. Lee, D. Lashkari, D. Shalon, P. O. Brown, and D. Botstein, "Distinctive gene expression patterns in human mammary epithelial cells and breast cancers," *Proc. Nat. Acad. Sci.*, vol. 96, pp. 9212–9217, 1999.
[17] M. B. Eisen, P. T. Spellman, P. O. Brown, and D. Botstein, "Cluster analysis and display of genome-wide expression patterns," *Proc. Nat. Acad. Sci.*, vol. 95, pp. 14 863–14 868, 1998.
[18] U. Alon, N. Barkai, D. A. Notterman, K. Gish, S. Ybarra, D. Mack, and A. J. Levine, "Broad pat-terns of gene expression revealed by clustering analysis of tumor and normal colon tissues probed by oligonu-cleotide arrays," *Proc. Nat. Acad. Sci.*, vol. 96, pp. 6745–6750, 1999.
[19] T. Golub, D. Slonim, P. Tamayo, C. Huard, M. Gaasenbeek, J. Mesirov, H. Coller, M. Loh, J. Dowing, M. Caligiuri, C. Bloomfield, and E. Lander, "Molecular classification of Cancer: Class discovery and class prediction by gene expression monitoring," *Science*, vol. 286, pp. 531–537, 1999.
[20] Y. H. Yang, M. J. Buckley, S. Dodoit, and T. P. Speed, "Comparison of methods for image analysis on cDNA microarray data," *J. Computational Graphic Statist.*, vol. 11, pp. 108–136.
[21] V. Troitsky, P. Ghisellini, E. Pechkova, and C. Nicolini, "DNASER: II. Novel Surface Patterning for Biomolecular Microarray," *IEEE Trans. Nanobiosci.*, vol. 1, pp. 73–77, June 2002.

Claudio Nicolini was born in Udine, Italy. He received the Ph.D. degree in nuclear physics from the University of Padua, Padua, Italy, in 1967.

After serving as Adjunct Professor of Physics at the University of Bari, Bari, Italy, he moved for 16 years to the United States, and was at Brown University, Providence, RI, Massachusetts Institute of Technology, Cambridge, and Brookhaven National Laboratory, Upton, NY. He then moved to Temple University School of Medicine, Philadelphia, PA, where after a period of intensive biomedical training and research he became Associate Professor of Pathology and then Full Professor and Director of the Division of biophysics. In 1984, he was called for "Chiara Fama," as "eminent scientist," to the chair of Biophysics of the University of Genoa, Genoa, Italy, where he is presently chairman of the Biophysical M&O Sciences and Technologies. Since 1991, he is President of Polo Nazionale Bioelettronica and of the Fondazione Elba. He has authored more than 400 publications in international scientific journals, 28 patents, and 21 books. His main scientific activities concerned biophysics and cancer research.

Dr. Nicolini was Science advisor to the Prime Minister during 1984–1986. He pioneered bioelectronics and nanotechnology and received several awards and prizes.

Andrea Marco Malvezzi received the Laurea degree in physics from the University of Milano, Milan, Italy, in 1971.

He is Associate Professor of Physics at University of Pavia, Pavia, Italy. His current research interests include ultrafast laser-matter interaction and spectroscopic investigation in the visible EUV and XUV regions.

Alessandra Tomaselli received the Laurea degree in electronic engineering and the Ph.D. in electronics and computer sciences.

She is currently an Assistant Professor at the Department of Electronics of the University of Pavia, Pavia, Italy.

Davide Sposito was born in Taormina, Italy. He received the Laurea degree in biomedical engineering from the University of Pisa, Pisa, Italy, in 1997.

He is currently with Polo Nazionale Bioelettronica, Rome, Italy. His main research interest is in biomedical instrumentation development.

Giuseppe Tropiano was born in Catania, Italy. He received the Laurea degree in computer science from the University of Pisa, Pisa, Italy, in 1993.

He is currently with Polo Nazionale Bioelettronica, Rome, Italy. His main research interest is in the field of image processing and neural networks.

Enrico Borgogno was born in Ivrea, Italy. He received the Laurea degree in environmental engineering from the Politecnico of Torino, Torino, Italy, in 1996.

He is currently with Polo Nazionale Bioelettronica, Rome, Italy. His main research interest is in the field remote sensing and neural networks.